Electronic Supporting Information for

ROS-generating Rare-Earth coordination networks for photodynamic inactivation of *Candida albicans*

Agustín A. Godoy[a], María C. Bernini[a], Matías D. Funes[b], Maximiliano Sortino[c,d], Sebastián E. Collins[e] & Griselda E. Narda[a]

a Instituto de Investigaciones en Tecnología Química (INTEQUI), Área de Química General e Inorgánica "Dr. G. F. Puelles", Facultad de Química, Bioquímica y Farmacia, Universidad Nacional de San Luis, Ejercito de los Andes 950, 5700 San Luis, Argentina.

b INTEQUI-CONICET, Área Química Orgánica, Facultad de Química, Bioquímica y Farmacia, Universidad Nacional de San Luis, Almte. Brown 1450, 5700 San Luis, Argentina.

c Farmacognosia, Facultad de Ciencias Bioquímicas y Farmacéuticas, Universidad Nacional de Rosario, Suipacha 531, 2000 Rosario, Argentina.

d Centro de Referencia de Micología, Facultad de Ciencias Bioquímicas y Farmacéuticas, Universidad Nacional de Rosario, Suipacha 531, 2000 Rosario, Argentina.

e. Instituto de Desarrollo Tecnológico para la Industria Química (INTEC), Universidad Nacional del Litoral, CONICET, Güemes 3450, S3000GLN, Santa Fe, Argentina.

Contents

Section S1 Inductively Coupled Plasma - Atomic Emission Spectroscopy (ICP-AES).

Table S1 ICP-AES measurements of **I-IV** systems.

Systems	% Y	% Tb	[CNs]		[ ] of systems **I-IV** in spectroscopic ROS determination experiments
			mM	ppm	ppm
I	100.00	0.00	1.24E-01	26.4	5.28
II	94.86	5.14	5.74E-02	12.67	2.53
III	100.00	0.00	4.41E-02	9.39	1.88
IV	94.50	5.50	5.52E-02	12.19	2.44

Section S2 Powder X-Ray Diffraction (PXRD) Refinements.

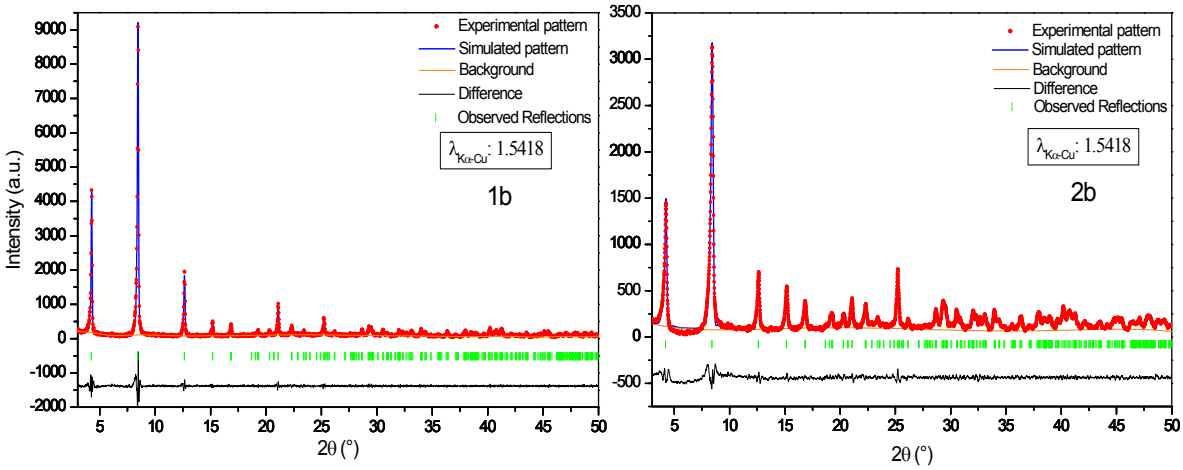

Figure S1 Pawley refinements for compounds **1b** and **2b**.

Table S2 Pawley refinement values for compounds **1b** and **2b**.

Compound	1b	2b
Lattice Type	Monoclinic	
Space Group	P21/c	
Rwp	13.91%	1.46%
Rp	10.76%	0.97%
Parameters		
a	21.127(2)	21.114(2)
b	6.1010(5)	6.0927(5)
c	7.6282(7)	7.6227(6)
β	92.367(8)	92.439(7)

Section S3 Fourier-Transform Infrared Spectroscopy (FTIR).

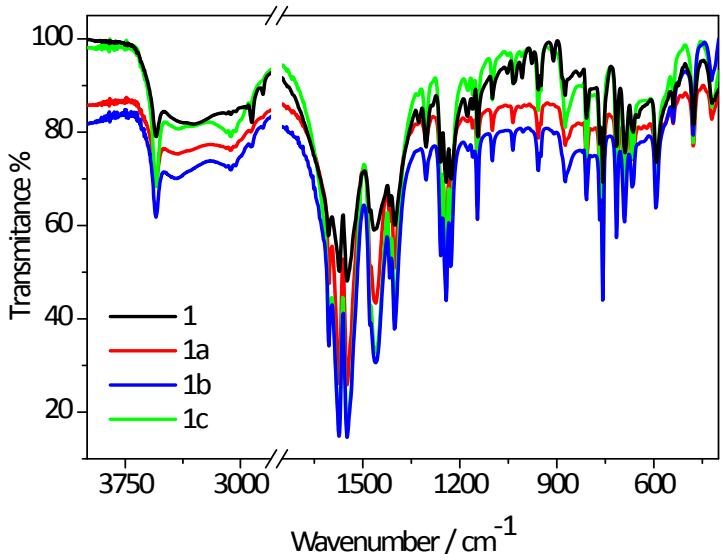

Figure S2 FTIR spectra of compounds **1**, **1a**, **1b** and **1c**. Wavenumber range between 400 and 4000 cm^{-1}. The spectra show the isostructural character in the series of compounds with formula **[Y(Salicylate)(Succinate)$_{0.5}$(H$_2$O)]** + *a* mg CTAB (*a* = 0, 100, 200 and 400) according to the functional groups present in each structure.

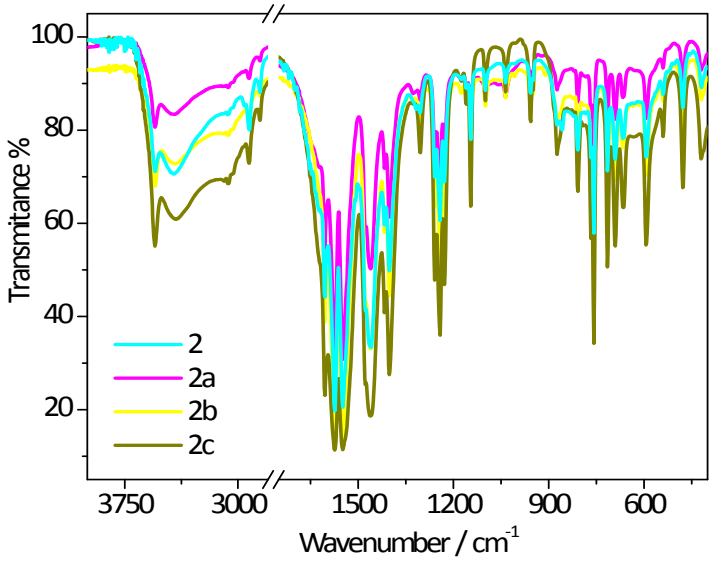

Figure S3 FTIR spectra of compounds **2**, **2a**, **2b** and **2c**. Wavenumber range between 400 and 4000 cm^{-1}. The spectra show the isostructural character in the series of compounds with formula **[Y$_{0.95}$Tb$_{0.05}$(Salicylate)(Succinate)$_{0.5}$(H$_2$O)]** + *a* mg CTAB (*a* = 0, 100, 200 and 400) according to the functional groups present in each structure.

Table S3 FTIR spectra assignment of series 1 and 2.

Wavenumber (cm^{-1})								Assignment
1	**1a**	**1b**	**1c**	**2**	**2a**	**2b**	**2c**	
3548 (m)	3548 (m)	3550 (m)	3548 (m)	3549 (m)	3549 (m)	3548 (m)	3549 (m)	**ν_{as}OH W**
3302 (br, w)	3411 (br, w)	3417 (br, w)	3407 (br, w)	3425 (br, w)	3422 (br, vw)	3419 (br, vw)	3410 (br,w)	
2925 (w)	2931 (vw)	2928 (vw)	2931 (vw)	2926 (vw)	2926 (vw)	2924 (w)	2926 (w)	**ν_{as}C-H**
1606 (w)	1605 (m)	1605 (m)	1605 (m)	1605 (m)	1605 (m)	1605 (m)	1605 (m)	**νCC aromatic ring**
1573 (m)	1573 (s)	1573 (s)	1573 (s)	1573 (s)	1573 (s)	1573 (s)	1574 (s)	**ν_{as}OCO bidentate bridge**
1548 (m)	1548 (s)	1548 (s)	1548 (s)	1548 (s)	1548 (s)	1548 (s)	1548 (s)	**ν_{as}OCO quelate-bridge**
1463 (br,m)	1461 (br,m)	1461 (br,m)	1461 (br,m)	1461 (br,m)	1461 (br,m)	1461 (br,m)	1460 (br,m)	**νCC aromatic ring + CH_2**
1401 (m)	1401 (s)	1401 (s)	1401 (s)	1401 (s)	1402 (s)	1401 (s)	1402 (s)	**ν_sOCO**
1304 (m)	1304 (m)	1304 (m)	1304 (m)	1304 (m)	1304 (m)	1304 (m)	1304 (m)	**$\rho_w CH_2$**
1241 (m)	1241 (m)	1241 (m)	1241 (m)	1241 (m)	1241 (m)	1241 (m)	1241 (s)	**νC-O fenoxi**
1144 (m)	1144 (m)	1144 (m)	1144 (m)	1144 (m)	1144 (m)	1144 (m)	1144 (m)	**δCCC aromatic**
757 (m)	757 (m)	757 (m)	757 (m)	757 (m)	757 (m)	757 (m)	757 (s)	**ρ_rC-H + o-disubstituted**

Section S4 Thermogravimetric Analysis (TGA).

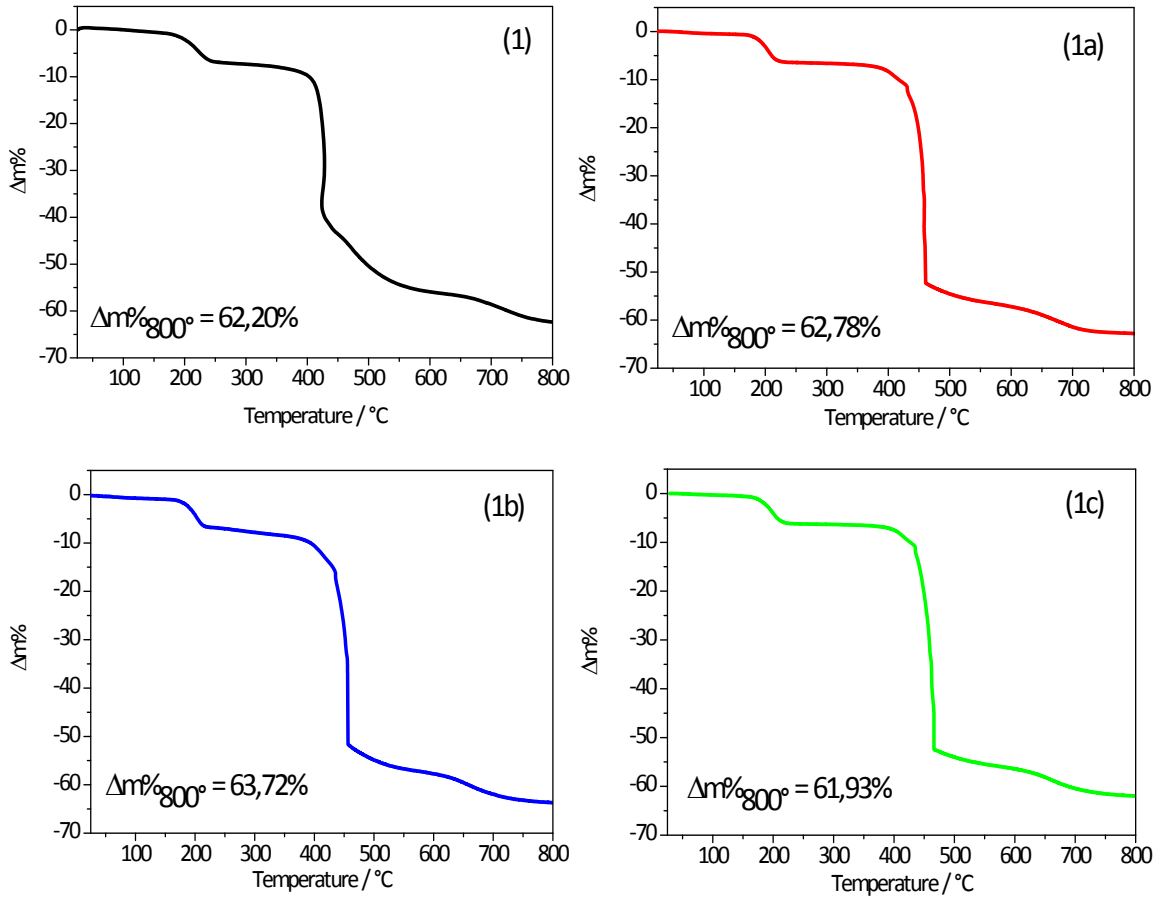

Figure S4 TGA of compounds **1**, **1a**, **1b** and **1c**. Heating range 25 to 800 ° C, air atmosphere. Heating rate 10 °C·min^{-1}. Thermogravimetric analysis shows the same decomposition events in all samples: coordinated water loss at approximately 200 ° C; decomposition of the organic structure from 450 ° C; total loss of mass at 800 ° C of 60%. The isostructural character of the series was corroborated by this technique.

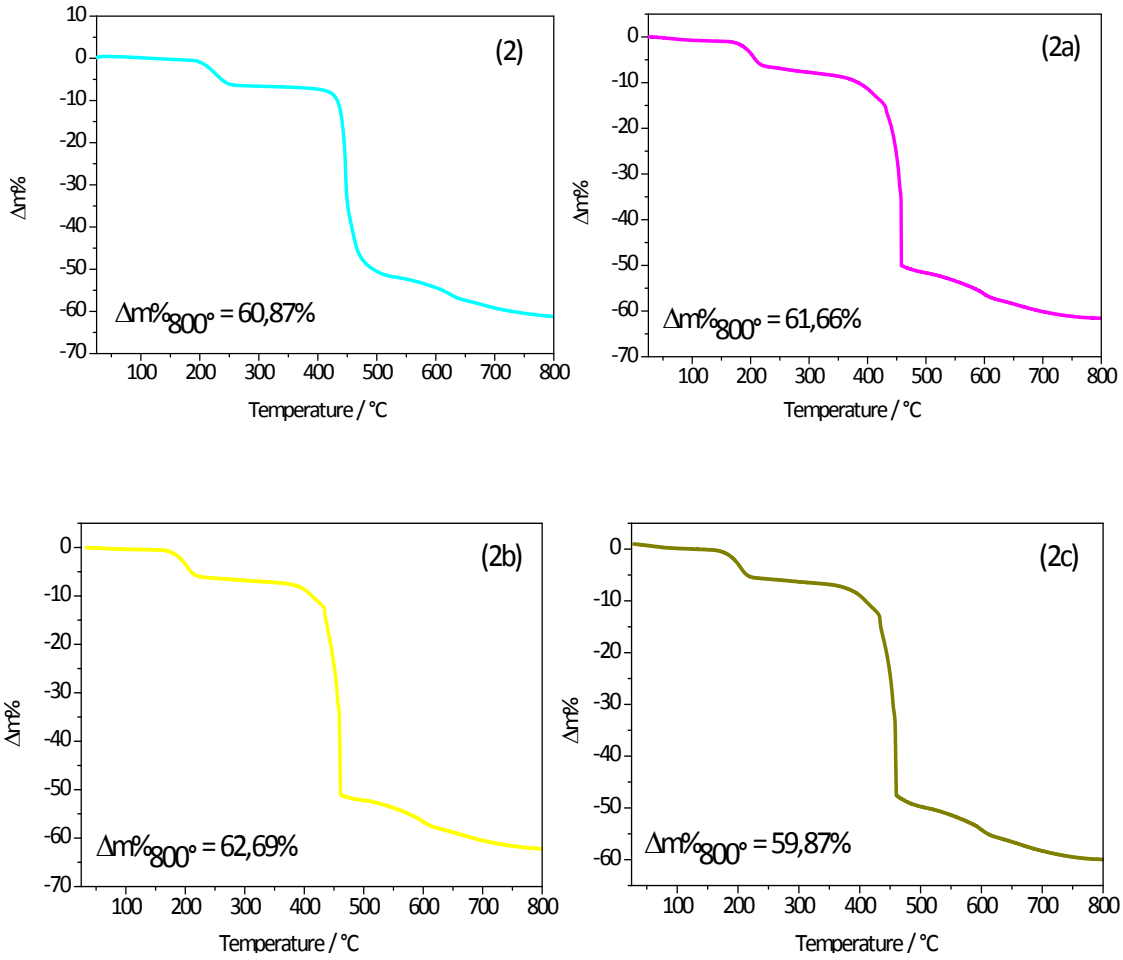

Figure S5 TGA profiles of compounds **2**, **2a**, **2b** and **2c**. Heating range 25 to 800 ° C, air atmosphere. Heating rate 10 °C·min^{-1}. Thermogravimetric analysis shows the same decomposition events in all samples: coordinated water loss at approximately 200 ° C; decomposition of the organic structure from 450 ° C; total loss of mass at 800 ° C of 60%. The isostructural character of the series was corroborated by this technique.

Section S5 Scanning Electron Microscopy (SEM).

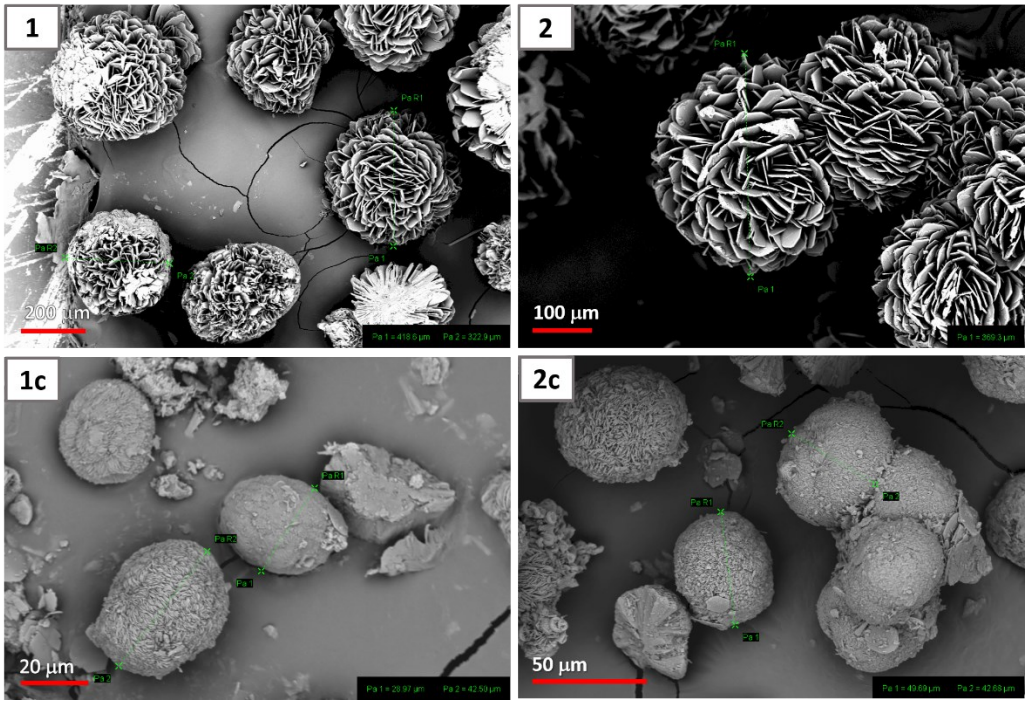

Figure S6-a SEM micrographs - Determination of aggregate size in secondary morphology. In these images, compounds **1** and **2** exhibit diameters in the range of 320-420 nm, while compounds **1c** and **2c** show a decrease in secondary morphology by a factor of 10, showing diameters in the range of 28 to 50 nm.

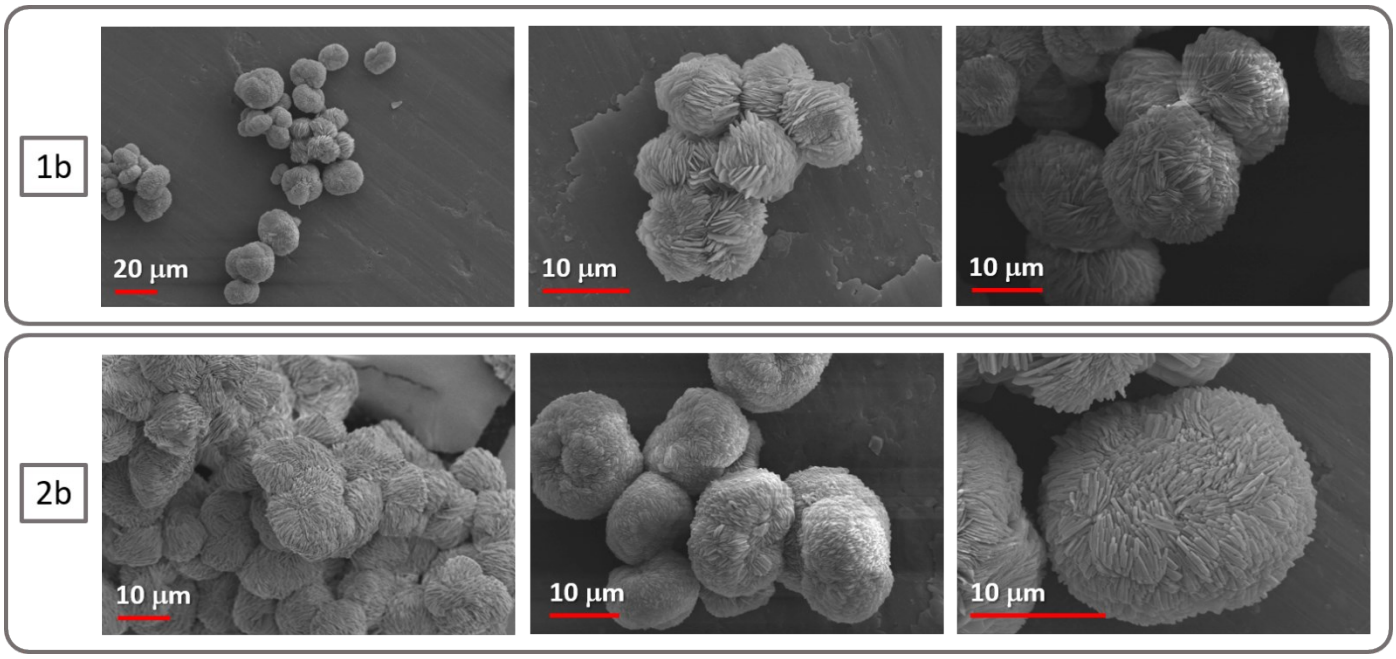

Figure S6-b SEM images of compounds **1b** and **2b**. Samples selected for post-synthesis treatments (top-down) and spectroscopic tests due to homogeneity in morphology and absence of secondary crystalline phases.

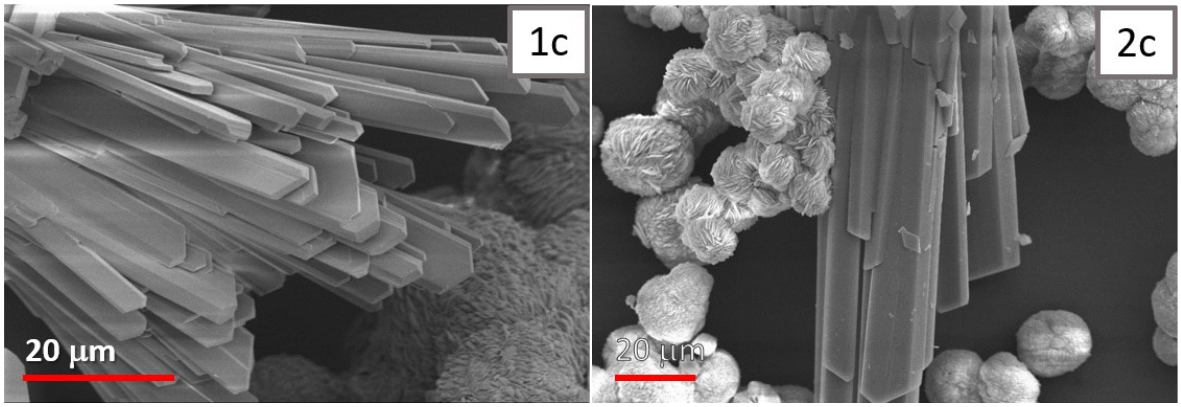

Figure S6-c SEM micrographs of high size single-crystals in **1c** and **2c** compounds. In addition to the primary and secondary morphologies, observed in the series of compounds **1**, **1a**, **1b**, **2**, **2a** and **2b**, the micrographs of compounds **1c** and **2c** present aggregates whose morphology corresponds to large prisms, for which they were discarded for further applied to the top-down approach.

Section S6 Transmission Electron Microscopy (TEM).

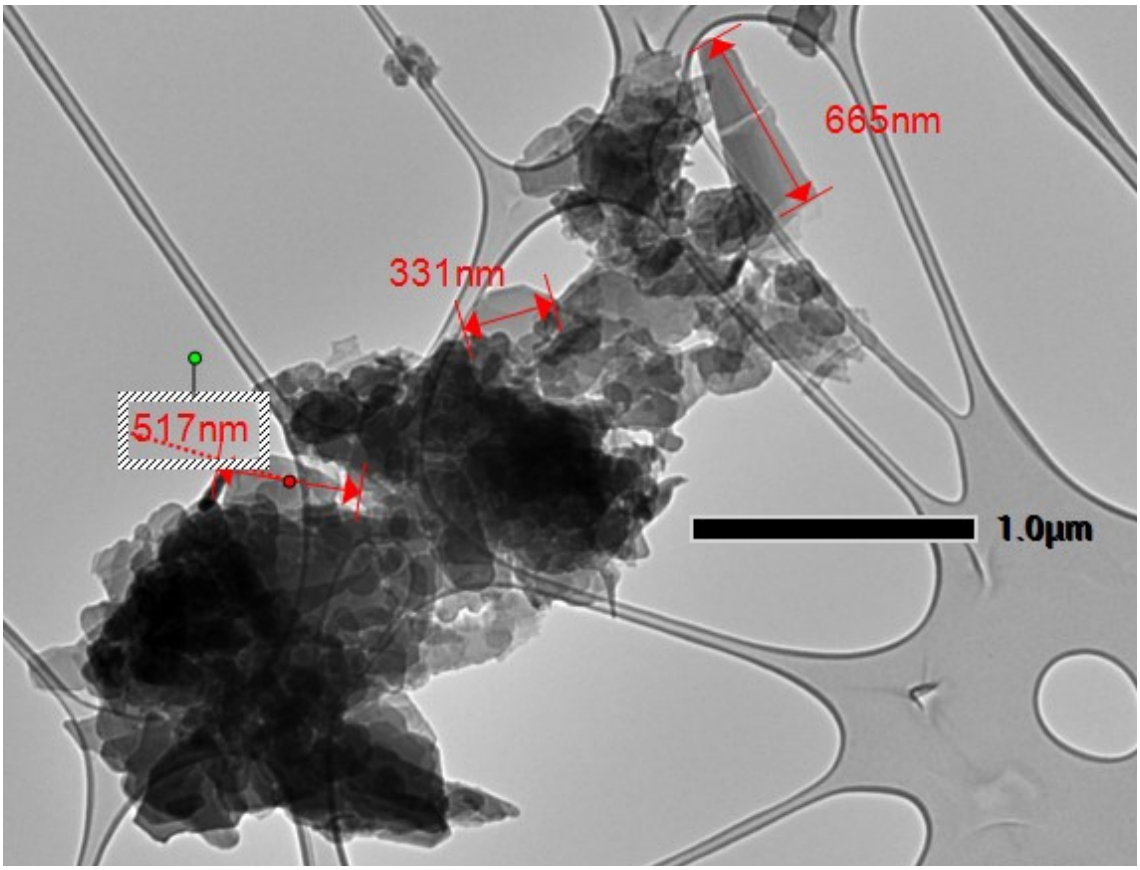

Figure S7-a Transmission electron microscopy (TEM) images of compound **2** resultant from 30 min of ultrasonication treatment of ethanol- suspension. Lengths and widths of selected particles are shown in red.

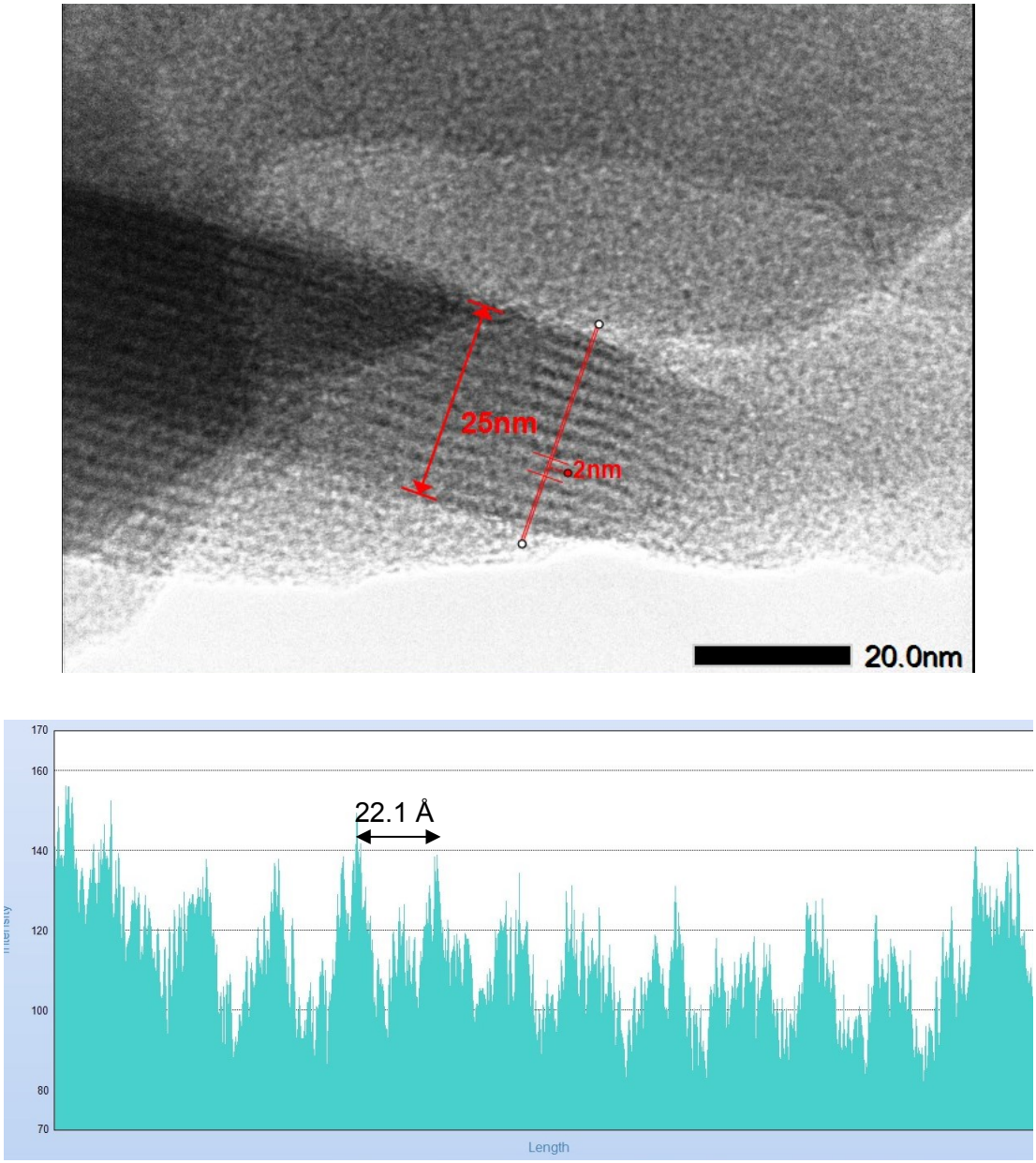

Figure S7-b Transmission electron microscopy (TEM) image of compound **2** (top) and intensity profile along the segment signed with red row (down).

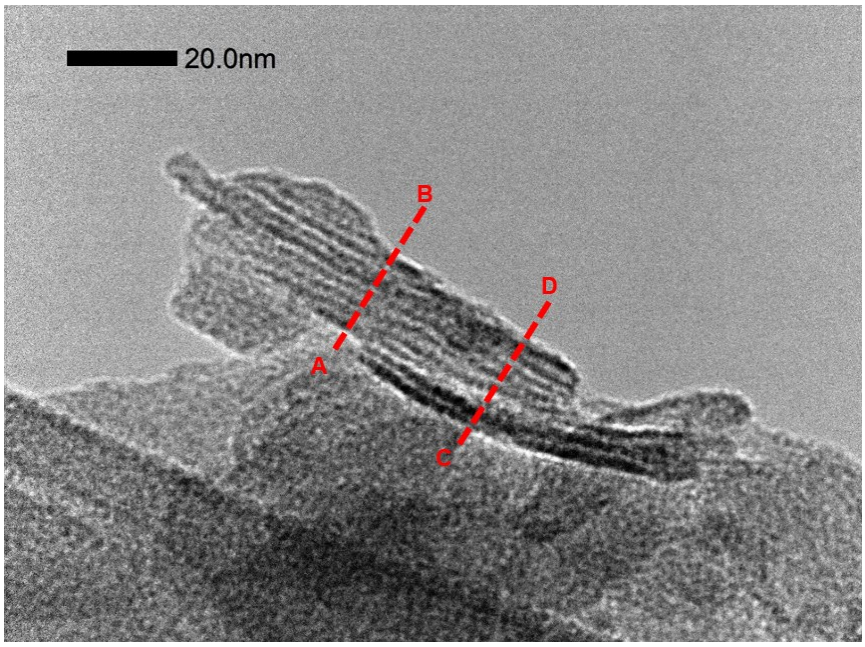

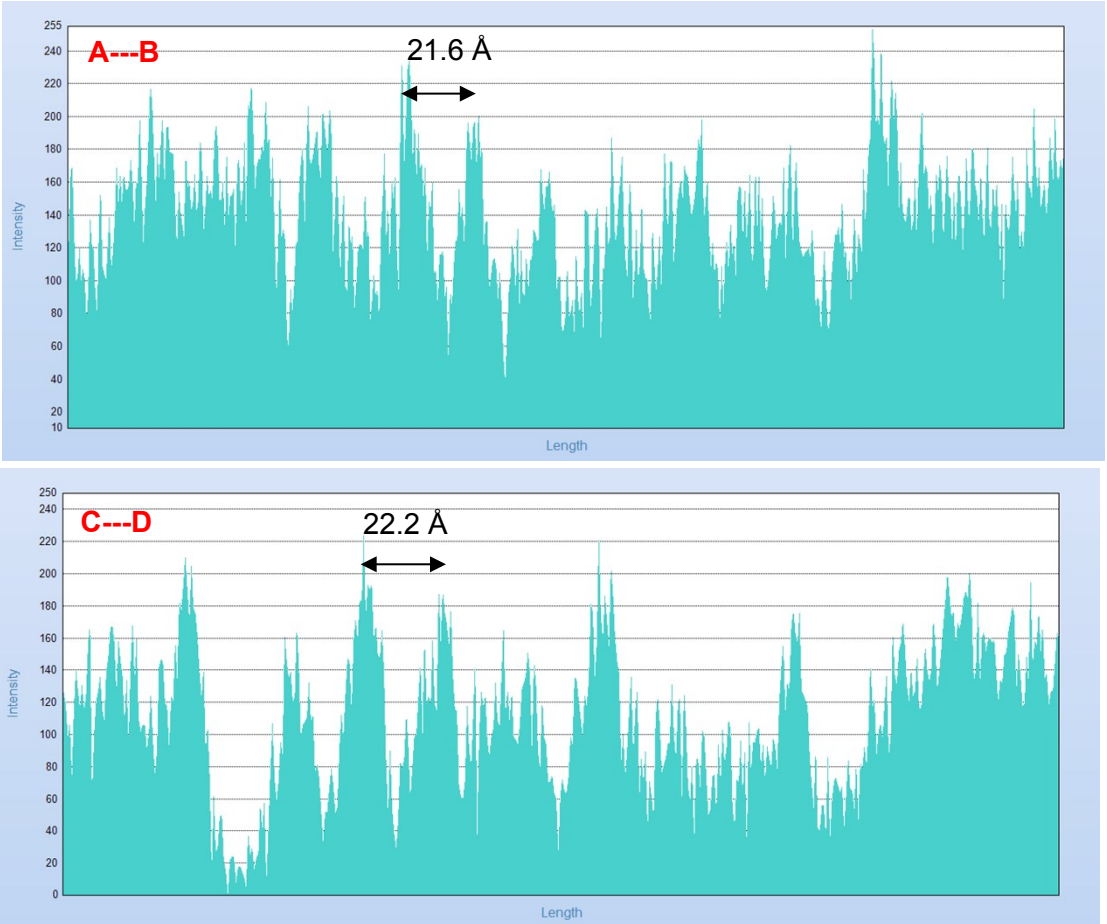

Figure S7-c Transmission electron microscopy image of nanoparticles of Sample **2c**. Intensity profiles along the trayectories A-B and C-D.

Section S7 Absorption and Fluorescence spectra of **I**-**IV** + Trp suspensions.

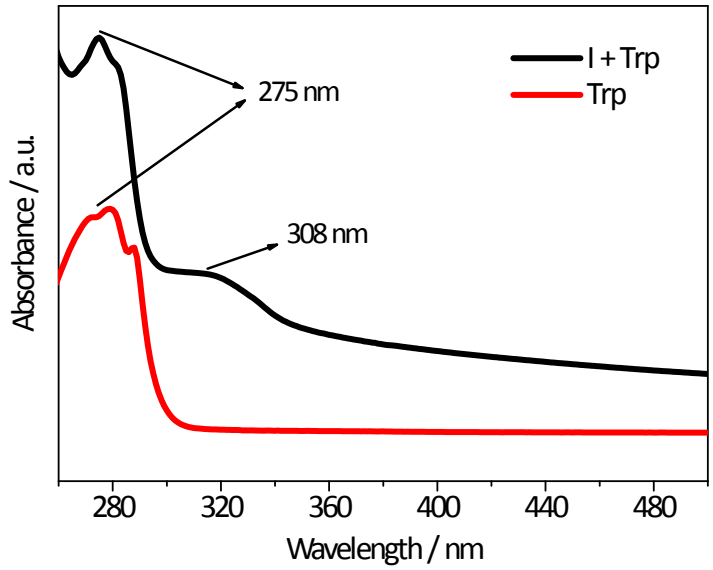

Figure S8 Full range absorption irradiation between 260-500 nm. As an example, **I** + Trp system was included in the description. The characteristic absorption band of Trp is shown in both cases with a maximum centered at 275 nm, subsequently determined as the excitation wavelength for fluorescence experiments. The salicylate absorption band for system I, centered at 308 nm is shown in system **I** + Trp.

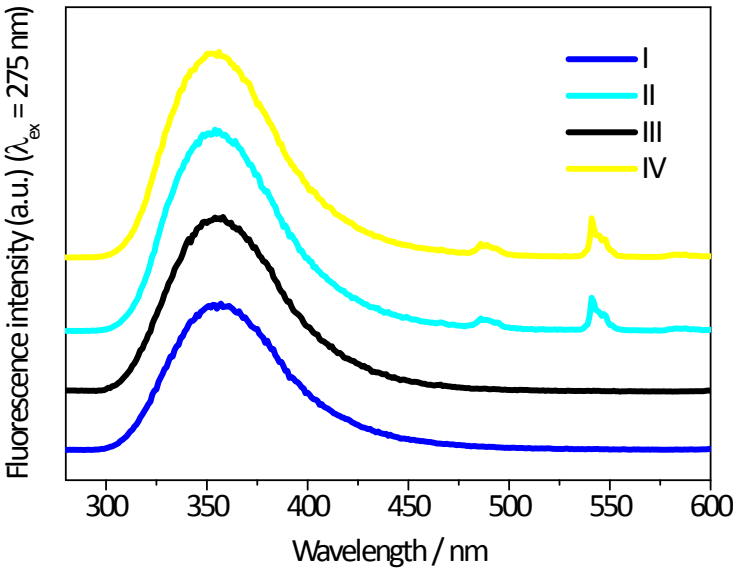

Figure S9 Full range fluorescence emission spectra of **I**-**IV** + Trp suspensions between 280-600 nm under excitation with 275 nm. Trp characteristic emission band centered at 355 nm and Tb^{3+} ion emission bands in systems **II** and **IV**. Emission signals of the salicylate ligand cannot be seen due to overlap with the high emission band of Trp.

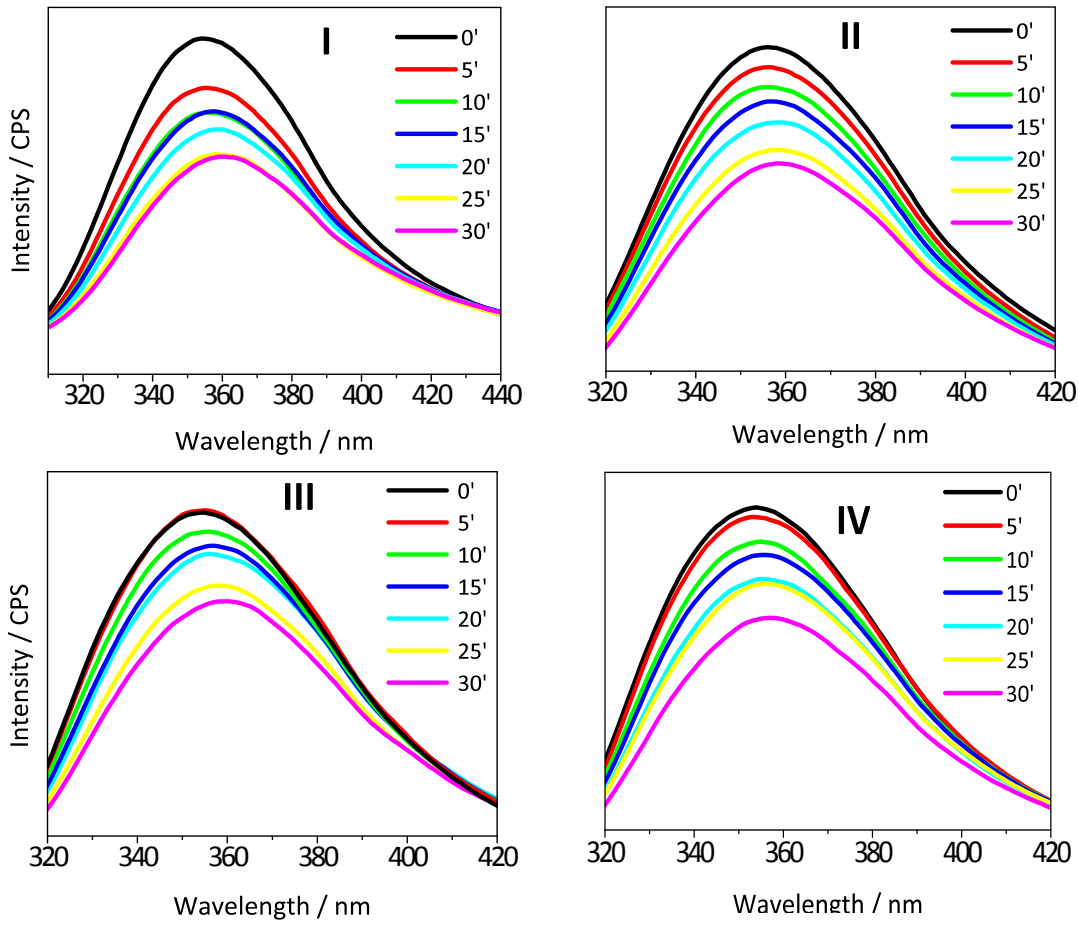

Figure S10 Time-dependence of fluorescence spectra of **I**-**IV** + Trp suspensions in the range 320-420 nm. After irradiation with 275 nm, decreasing of maximum fluorescence band of Trp, centered in 355 nm, was monitored between 0 and 30 minutes.

Section S8 Photolysis experiments of 1,3-DPBF.

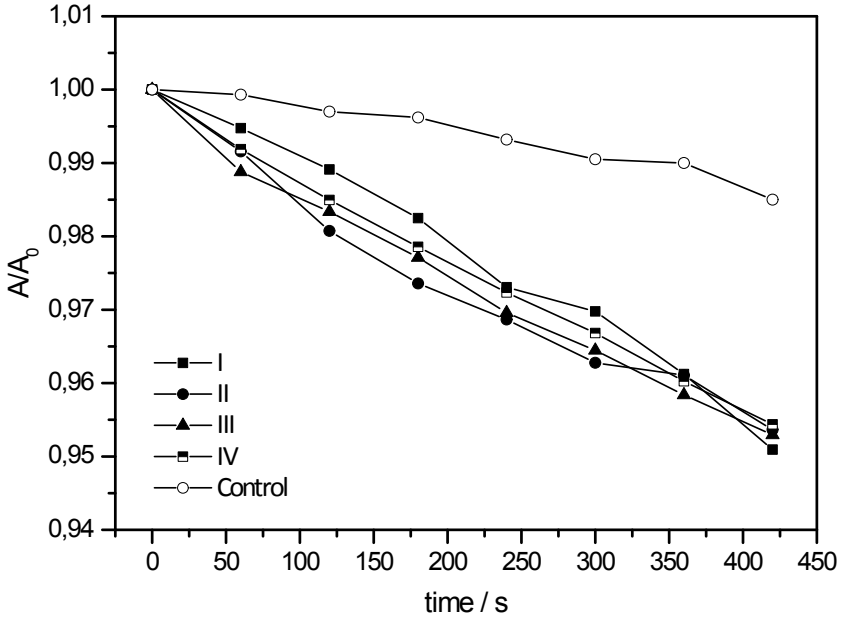

Figure S11 Relative absorbance vs. time of 1,3-DPBF against **I-IV** systems. Decrease in relative absorbance, monitored at 410 nm, over a 15 minute interval. 1,3-DPBF methanol solution (2.5 ml, 50 mM) is included as a control to compare with systems **I**-**IV**.